






Dimensional Synthesis for the Chang'e-Type Legged Mobile Lander Based on Performance Atlas

Youcheng Han  and Weizhong Guo  

State Key Laboratory of Mechanical Systems and Vibration,
School of Mechanical Engineering, Shanghai Jiao Tong University,
Shanghai, China

{youcheng, wzguo}@sjtu.edu.cn

Abstract. Legged mobile lander (LML) possesses both landing and walking functions with the promising application prospect in extraterrestrial exploration. There are three challenges on the dimensional synthesis method for the LML, including the derivation of the performance criteria for both landing and walking behaviors, the establishment of the dimensional optimization design model, and the demonstration and expression method for dimensional synthesis. To solve these problems, the paper will firstly introduce the mechanism topology of the proposed Chang'e-Type LML; then, derive the optimization parameters and the optimization criteria; thereafter, implement the non-dimensional optimization process for both single leg and overall robot respectively by the performance atlas approach; finally, obtain the dimensional global optimum solution. The study can help one understand the relationship between different dimensions and the corresponding performances, and obtain the global optimum dimensions for the Chang'e-Type LML.

Keywords: Legged mobile lander · Dimensional synthesis · Performance atlas · Optimization design · Chang'e

1 Introduction

Recently, extraterrestrial exploration has become a hot topic, and many schemes for the exploration system are proposed by academic institutes, commercial organizations, and aerospace agencies. The lander carrying with the rover is recognized as a conventional method applied among different nations, such as American's Apollo Project (1969–1972) [1], Soviet/Russian's LK Lunar Craft Program (1970–1971) [2], Chinese Chang'e 3 & 4 Program (2013–2019) [3] and so on. On the other hand, the mobile landing exploration robot is proposed with both landing and walking functions, which is also designed with complicated mechanism and structure, such as the robotic and crewed centaur lander by Lockheed Martin [4], the Mars cargo lander by Boeing Company [5], the wheel-legged mobile manned lunar lander by China Academy of Space Technology [6] and so on. In this paper, we propose a new legged mobile lander (LML) with the similar mechanism topology of Chang'e 3 & 4 lunar lander, and

commit to implement the dimensional synthesis of the Chang'e-Type LML with the best landing and walking performances.

As shown in the previous researches [7–9], the structural design method is widely used for the past legged landers, which takes the lander as truss structure with buffering characteristics, then investigates the structural strength, reliability, finite element analysis, etc. All that matters is there is not a cogent approach to determine the preliminary dimensions of the truss structure, which depends on the experience and intuition of designers. Moreover, the evaluation indices for both landing and walking behaviors are not sufficient and reasonable at present. Most criteria are suited to the analysis or test process rather than the design process, such as the four statistical landing performance criteria used in Apollo Project [10] and the five comprehensive evaluation indices used in Chang'e 3 Program [7] are all applied in landing tests. Furthermore, the demonstration and expression method for dimensional synthesis is of vital importance as well. For a long time, the cost function approach is widely used by the multi-object numerical algorithm, for instance, Wu et al. [11] utilize the second generation of non-inferior sorting genetic algorithm to optimize the legged lander with multiple objections. However, this approach is easy to get a local optimum solution, or else it requires more computing time and effort to get the global optimum solution. Furthermore, it's still not perceptual to compare different solutions by visualization, and the designers don't know the optimal degree of optimization results.

In conclusion, there is almost no directly feasible method for the dimensional synthesis of the LML at present. Hence, the paper is structured as follows: Step 1, introduces the mechanism topology of the proposed Chang'e-Type LML; Step 2, derives the optimization parameters and the optimization criteria; Step 3, demonstrates the non-dimensional optimization process of both single leg and overall robot respectively with the performance-chart based design methodology (PCbDM); Step 4, obtains the dimensional global optimum solution of the Chang'e-Type LML.

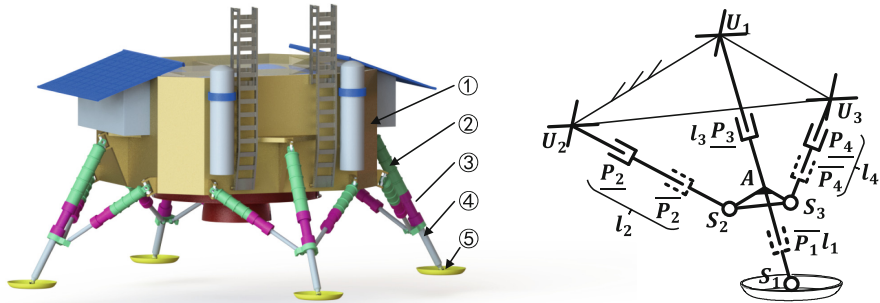
2 Structure and Optimization Criteria

2.1 Structure and Mechanism

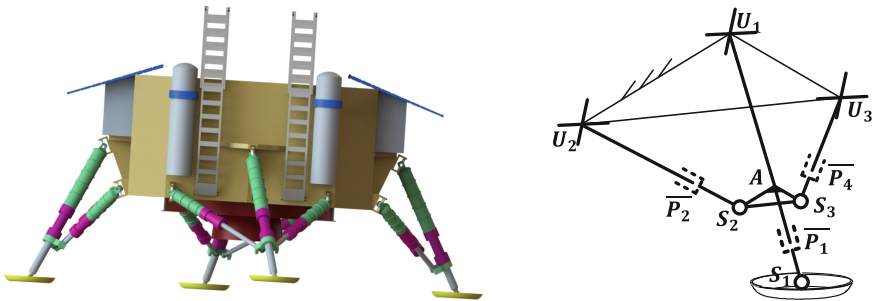
Figure 1 shows the structure and mechanism of the LML among different stages. The LML contains one main body and four legs with both landing and walking functions. Each limb in the leg includes one actuation sleeve, one damper sleeve, and one damper piston. Their coupling relationships are illustrated in the figure detailedly, where U denotes the universal hinge, S denotes the spherical hinge, \underline{P} denotes the prismatic hinge between the actuation sleeve and the damper sleeve, while \bar{P} denotes the equivalent prismatic hinge for the damper when it's shortened or stretched by landing impact. In pre-landing stage, the LML can be seen as a truss structure with zero mobility. In landing stage, the damper in main limb is shortened while the damper in secondary limb is both possible to be shortened or stretched under different landing conditions, so the single leg is recognized as the hybrid mechanism $(2U\bar{P}\&U) - \bar{P}$

with 2R1T motion characteristics. In walking stage, all dampers are fixed with constant lengths. The damper sleeve is actuated by the actuation sleeve, so the single leg is recognized as the parallel mechanism $2UPS\&UP$ with 2R1T motion characteristics.

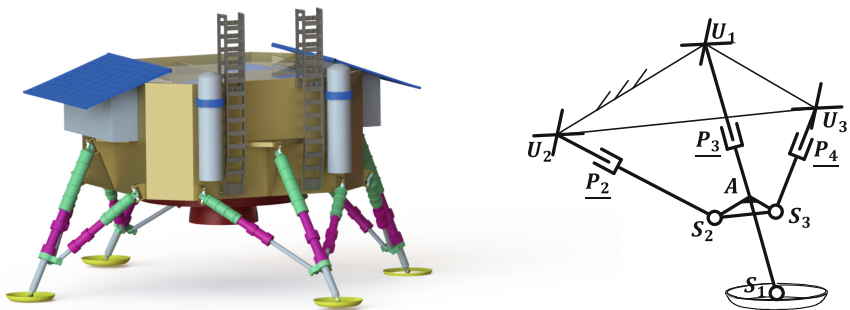
In this figure, $l_1 + l_3$ represents the length of main limb, l_2 and l_4 represent two secondary limbs. For the single leg, the static platform isosceles triangle $\Delta U_1U_2U_3$ is similar to the moving platform isosceles triangle ΔAS_2S_3 , their bottom edges are $|U_2U_3| = 2a_1$ and $|S_2S_3| = 2a_2$, heights are b_1 and b_2 . Moreover, the main body is a $2d \times 2d \times d$ cuboid, θ_{in} is the installation angle between single leg and main body.



(a) pre-landing stage: structure and mechanism



(b) landing stage: structure and mechanism



(c) walking stage: structure and mechanism

- ① main body; ② actuation sleeve; ③ damper sleeve; ④ damper piston; ⑤ footpad

Fig. 1. Structure and mechanism of the LML among different stages

There are five optimization parameters for the single leg, including a_1, b_1, a_2, b_2, l_3 , and three optimization parameters for the overall robot, including l_3, R_{ms}, R_{sp} , where R_{ms} represents the distance between the main body axis and the main strut universal hinge, which can be considered as the radius of the moving platform of the LML, $R_{ms} = d + b_1 \sin \theta_{in}$; R_{sp} represents the radius of the circle formed by four footpads, which can also be considered as the radius of the static platform of the LML.

2.2 Optimization Criteria

There are five performance indices for evaluating the landing and walking behaviors of the LML shown in Table 1, where “★” denotes the index is appropriate for the single leg or overall robot. Among them, the first four indices are based on the works by Gosselin, and Liu, etc. [12, 13], while the fifth index is first put forward based on the work by Papadopoulos [14].

Table 1. Performances indices for single leg and overall robot

Types	Leg	LML	Expression
WVI	★	★	$\eta_W = \int_0^{2\pi} d\theta \int_0^{\rho_{max}} \rho d\rho \int_{z_{min}}^{z_{max}} dz$ (1)
GCI	★	★	$\eta_{Jv} = \frac{\int_V \mu_{Jv} dW}{\int_V dW}$ (2)
		★	$\eta_{J\omega} = \frac{\int_V \mu_{J\omega} dW}{\int_V dW}$ (3)
GPI	★	★	$\eta_{Fmax} = \frac{\int_V \sqrt{\max(\lambda_{Fi})} dW}{\int_V dW}, \eta_{Fmin} = \frac{\int_V \sqrt{\min(\lambda_{Fi})} dW}{\int_V dW}$ (4)
		★	$\eta_{Mmax} = \frac{\int_V \sqrt{\max(\lambda_{Mi})} dW}{\int_V dW}, \eta_{Mmin} = \frac{\int_V \sqrt{\min(\lambda_{Mi})} dW}{\int_V dW}$ (5)
GSI	★	★	$\eta_{Pmax} = \frac{\int_V \sqrt{\max(\lambda_{Pi})} dW}{\int_V dW}, \eta_{Pmin} = \frac{\int_V \sqrt{\min(\lambda_{Pi})} dW}{\int_V dW}$ (6)
		★	$\eta_{Omax} = \frac{\int_V \sqrt{\max(\lambda_{Oi})} dW}{\int_V dW}, \eta_{Omin} = \frac{\int_V \sqrt{\min(\lambda_{Oi})} dW}{\int_V dW}$ (7)
GLSI		★	$\eta_S = \frac{\int_V S_k dW}{\int_V dW}, S_k = \min(\theta_i \cdot \ \mathbf{d}_i\ \cdot \ \mathbf{F}_i^*\)$ (8)

In the table, the workspace volume index (WVI) represents the buffering extent and ability and is the basis to establish all other performances; the global conditioning index (GCI) evaluates the dexterity, isotropy and the ability away from singularity; the global payload index (GPI) evaluates the extremum of the force or moment in landing and walking stages; the global stiffness index (GSI) evaluates the linear and angular displacement deformation; the global landing stability index (GLSI) evaluates both

horizontal and vertical stabilities to make the landing or walking stage secure. Furthermore, we hope a bigger WVI, bigger GCIs, bigger GPIs, smaller GSIs and bigger GLSI for the LML as the best multi-objective performances. In the following, to balance all these performance criteria, we'll transform the multi-objective optimization problem into the single-objective optimization problem to implement the dimensional synthesis process.

3 Non-dimensional Optimization of the Single Leg

For the single leg, the dimensional synthesis problem can be abstracted into the dimensional optimization design model as follows:

$$\left\{ \begin{array}{l} \text{Parameters: } X_{LEG} = \{a_1, b_1, a_2, b_2, l_3\} \\ \text{Maximum: } F(X_{LEG}) = m_1\tilde{\eta}_W + m_2\tilde{\eta}_{Jv} + m_3\tilde{\eta}_{Fmax} + m_4\tilde{\eta}_{Fmin} \\ \quad + m_5(1 - \tilde{\eta}_{Pmax}) + m_6(1 - \tilde{\eta}_{Pmin}) \\ \text{Subject to: } \left\{ \begin{array}{l} l_{imin} \leq l_{ji} \leq l_{imax} \\ \beta_{min} \leq \beta_{ji} \leq \beta_{max} \\ \gamma_{min} \leq \gamma_{ji} \leq \gamma_{max} \\ \xi_{min} \leq \xi_{ji} \leq \xi_{max} \end{array} \right. \end{array} \right. \quad (9)$$

where $\tilde{\eta}_i$ ($i \in [1, 6]$) is the normalization form of η_i , and $\tilde{\eta}_i \in [0, 1]$; m_i is the effective weighting factor of $\tilde{\eta}_i$ to construct the single-objective optimization problem, and $\sum m_i = 1$. Moreover, the constraint conditions are the angle ranges of $\beta_{ji}, \gamma_{ji}, \xi_{ji}$ for universal and spherical hinges, and the lengths ranges of l_{ji} for dampers.

Based on the PCbDM method, the normalized equation can be obtained by:

$$r_1 + r_2 + r_3 + r_4 + r_5 = 5 \quad (10)$$

where $r_1 = l_3/R$, $r_2 = b_1/R$, $r_3 = b_2/R$, $r_4 = a_1/R$, $r_5 = a_2/R$, and R is the normalization factor. Considering that the low DOF parallel mechanism usually owns the geometrically similar static platform and moving platform to get better performances [15], hereby we let $r_4/r_2 = r_5/r_3 = \chi$, and assign $\chi = 1.5$ on account of the supporting stiffness and landing stability. Equation (11) indicates the parameter design space, which is illustrated in Fig. 2 by the rectangular pyramid $ABCDE$.

$$r_1 + (1 + \chi)(r_2 + r_3) = 5 \quad (11)$$

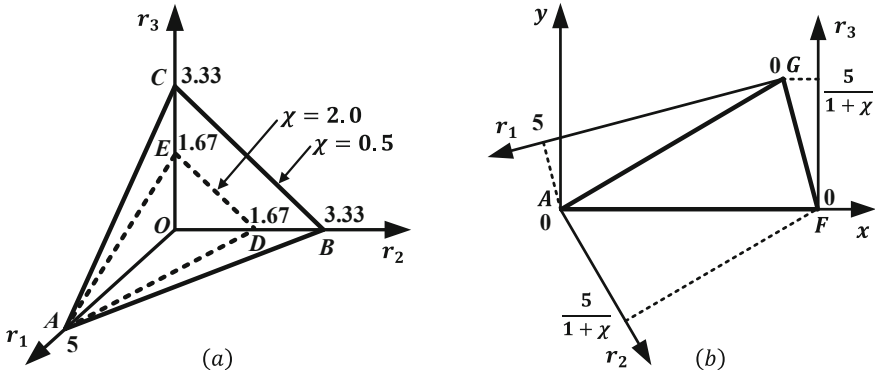


Fig. 2. Parameter design space of the single leg

Figure 3 shows the comprehensive performance atlas of the single leg, where $m_1, m_2, m_4, m_5 = 0.2$, and $m_3, m_6 = 0.1$. One can see that: (1) the comprehensive performance in the design space is almost inversely proportional to r_3 when r_1 is specified, which means the dimensions of the moving platform of the single leg should be smaller than that of the static platform; (2) for the single leg with the best comprehensive performance, the optimum solution region is $\Omega_{LEG} = \{(r_1, r_2, r_3) | 2.0 < r_1 < 3.5, 0.6 < r_2 < 1.2, 0 < r_3 < 0.4\}$.

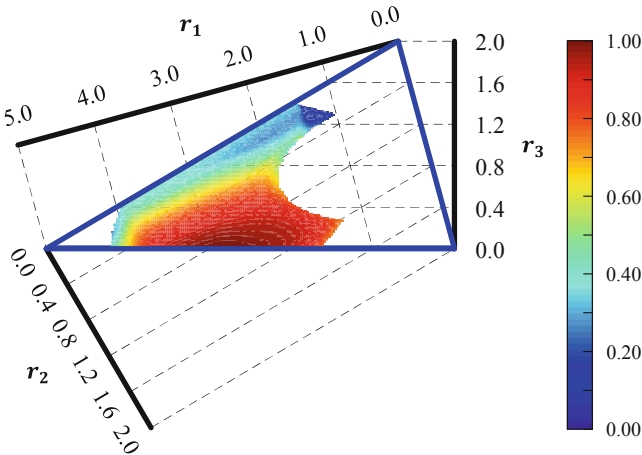


Fig. 3. Comprehensive performance atlas of the single leg

Table 2 gives the numerical analysis for the multi-objective performances of the single leg, and lists ten different dimension combinations and the corresponding performances in Ω_{LEG} . For the reason that there is not a unique optimum solution for the multi-objective optimization problem, and it relies on the designer to decide the importance degree of different performance indices. By contrast, we determine to

choose No. 8 as the optimum non-dimensional parameters for the following investigation, to get a better landing and walking performances.

Table 2. Numerical analysis for the multi-objective performance of the single leg

No.	(r_1, r_2, r_3)	$(\eta_W, \eta_{Jv}, \eta_{Fmax}, \eta_{Fmin}, \eta_{Pmax}, \eta_{Pmin})$
1	(2.00,0.80,0.40)	(0.40,0.61,1.10,0.67,2.42,0.88)
2	(2.00,0.90,0.30)	(1.13,0.62,1.23,0.74,2.03,0.78)
3	(2.00,1.00,0.20)	(2.65,0.60,1.42,0.79,1.81,0.68)
4	(2.00,1.10,0.10)	(5.28,0.57,1.59,0.80,1.76,0.61)
5	(2.50,0.60,0.40)	(15.55,0.50,1.48,0.66,3.21,0.77)
6	(2.50,0.70,0.30)	(14.13,0.53,1.58,0.72,2.44,0.71)
7	(2.50,0.80,0.20)	(15.03,0.53,1.70,0.76,2.08,0.61)
8	(2.50,0.90,0.10)	(17.06,0.52,1.83,0.79,1.88,0.57)
9	(3.00,0.60,0.20)	(37.29,0.46,1.70,0.66,3.75,0.69)
10	(3.00,0.70,0.10)	(37.10,0.47,1.84,0.72,2.83,0.62)

4 Non-dimensional Optimization of the Overall Robot

For the overall robot, the dimensional synthesis problem can be abstracted into the dimensional optimization design model as follows:

$$\left\{ \begin{array}{l}
 \text{Parameters: } X_{LML} = \{l_3, R_{ms}, R_{sp}\} \\
 \text{Maximum: } F(X_{LML}) = n_1\tilde{\eta}_W + n_2\tilde{\eta}_{Jv} + n_3\tilde{\eta}_{J\omega} + n_4\tilde{\eta}_{Fmax} + n_5\tilde{\eta}_{Fmin} \\
 \quad + n_6\tilde{\eta}_{Mmax} + n_7\tilde{\eta}_{Mmin} + n_8(1 - \tilde{\eta}_{Pmax}) + n_9(1 - \tilde{\eta}_{Pmin}) \\
 \quad + n_{10}(1 - \tilde{\eta}_{Omax}) + n_{11}(1 - \tilde{\eta}_{Omin}) + n_{12}\tilde{\eta}_S \\
 \text{Subject to: } \left\{ \begin{array}{l}
 L_v - [L_v] \geq 0 \\
 L_h - [L_h] \geq 0 \\
 L_{imin} \leq L_{ji} \leq L_{imax} \\
 \beta_{min} \leq \beta_{ji} \leq \beta_{max} \\
 \gamma_{min} \leq \gamma_{ji} \leq \gamma_{max} \\
 \xi_{min} \leq \xi_{ji} \leq \xi_{max}
 \end{array} \right.
 \end{array} \right. \tag{12}$$

where $\tilde{\eta}_i$ ($i \in [1, 12]$) is the normalization form of η_i , and $\tilde{\eta}_i \in [0, 1]$; n_i is the effective weighting factor of $\tilde{\eta}_i$ to construct the single-objective optimization problem, and $\sum n_i = 1$. Moreover, the constraint conditions are the landing stability constraints in both horizontal and vertical directions, the angle ranges of $\beta_{ji}, \gamma_{ji}, \xi_{ji}$ for universal and spherical hinges, the lengths ranges of L_{ji} for actuators, where L_v is the distance

between the engine nozzle skirt and the extraterrestrial surface, L_h is the distance between the main body axis and the connecting line of two adjacent footpads, $[L_v]$ and $[L_h]$ are the minimum value of L_v and L_h that ensure the LML secure.

Based on the PCbDM method, the normalized equation can be obtained by:

$$t_1 + t_2 + t_3 = 3 \tag{13}$$

where $t_1 = l_3/T$, $t_2 = R_{ms}/T$, $t_3 = R_{sp}/T$, and T is the normalization factor. Hence, Eq. (13) indicates the parameter design space, which is illustrated in Fig. 4 as well.

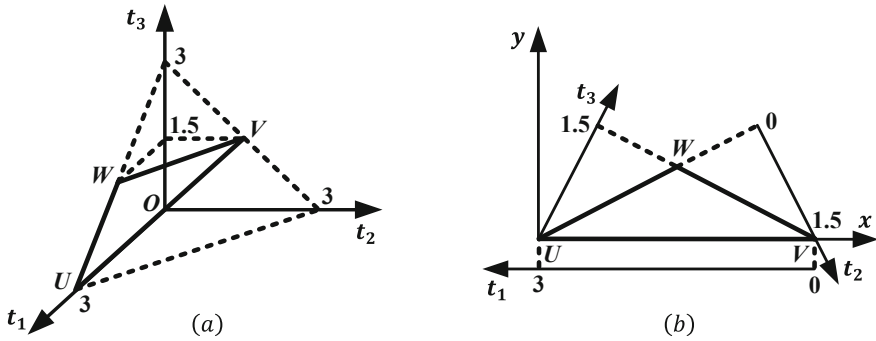


Fig. 4. Parameter design space of the overall robot

Figure 5 shows the comprehensive performance atlas of the overall robot, where $n_1, n_2, n_3, n_5, n_7, n_8, n_{10}, n_{12} = 0.1$, and $n_4, n_6, n_9, n_{11} = 0.05$. One can see that: (1) the comprehensive performance in the design space is almost proportional to t_3 when t_1 or t_2 is specified, which means R_{sp} should be bigger than R_{ms} . (2) for the overall robot with the best comprehensive performance, the optimum solution region is $\Omega_{LML} = \{(t_1, t_2, t_3) | 0.4 < t_1 < 1.6, 0 < t_2 < 1.1, 1.3 < t_3 < 1.5\}$.

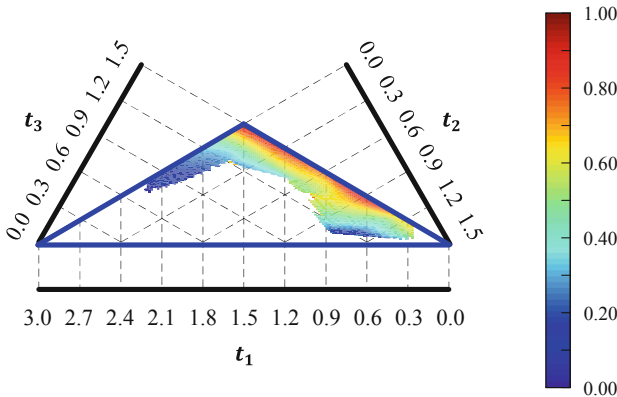


Fig. 5. Comprehensive performance atlas of the overall robot

Table 3 gives the numerical analysis for the multi-objective performances of the overall robot, and lists thirteen different dimension combinations and the corresponding performances in Ω_{LML} . By contrast, we determine to choose No. 2 as the optimum non-dimensional parameters, to get a better landing and walking performance.

Table 3. Numerical analysis for the multi-objective performance of the overall robot

No.	(t_1, t_2, t_3)	$(\eta_W, \eta_{Jv}, \eta_{J\omega}, \eta_{Fmax}, \eta_{Fmin}, \eta_{Mmax}, \eta_{Mmin}, \eta_{Pmax}, \eta_{Pmin}, \eta_{Omax}, \eta_{Omin}, \eta_S)$
1	(0.4,1.1,1.5)	(0.26,0.25,0.23,2.09,0.49,0.60,0.12,6.18,0.24,131.39,5.17,0.60)
2	(0.6,0.9,1.5)	(0.57,0.51,0.26,1.74,0.83,1.03,0.19,1.96,0.35,35.80,4.90,0.66)
3	(0.6,1,1.4)	(0.19,0.31,0.28,2.00,0.59,0.34,0.08,3.93,0.25,213.60,17.13,0.41)
4	(0.8,0.7,1.5)	(0.87,0.61,0.18,1.64,0.97,1.39,0.21,1.16,0.39,24.13,1.69,0.69)
5	(0.8,0.8,1.4)	(0.22,0.45,0.22,1.89,0.83,0.90,0.12,1.78,0.28,82.72,9.24,0.45)
6	(0.8,0.9,1.3)	(0.10,0.40,0.27,1.95,0.77,0.21,0.05,1.91,0.26,386.36,30.28,0.28)
7	(1,0.5,1.5)	(0.97,0.58,0.14,1.67,0.94,1.51,0.21,1.21,0.38,24.29,0.56,0.74)
8	(1,0.6,1.4)	(0.46,0.29,0.11,2.01,0.57,1.43,0.16,3.99,0.25,41.93,0.70,0.54)
9	(1.2,0.3,1.5)	(0.89,0.49,0.14,1.75,0.84,1.48,0.21,1.51,0.34,24.03,0.48,0.85)
10	(1.2,0.4,1.4)	(0.67,0.24,0.11,2.08,0.49,1.39,0.16,4.66,0.23,40.98,0.53,0.54)
11	(1.4,0.1,1.5)	(0.53,0.39,0.14,1.90,0.72,1.41,0.20,2.06,0.29,26.37,0.55,1.08)
12	(1.4,0.2,1.4)	(0.51,0.2,0.13,2.14,0.49,1.17,0.15,4.34,0.22,47.47,0.75,0.74)
13	(1.4,0.3,1.3)	(0.46,0.14,0.11,2.26,0.32,0.94,0.11,10.32,0.20,87.59,1.15,0.45)

5 Dimensional Global Optimum Solution

Given in the stowed stage, the LML should meet the envelope demand of the carrying vehicle, that is to say, the diameter of the LML should be less than the envelope diameter ϕ_e of the carrying vehicle, given by:

$$\max(2\sqrt{2}d, 2R_{ms}) < \phi_e \tag{14}$$

According to the equation $d = R_{ms} - b_1 \sin\theta_{in}$ and the non-dimensional parameters solved in Sects. 3 and 4, we can deduce $2\sqrt{2}d < \phi_e$. Here we take $\phi_e = 3650$ mm in reference to the envelope demand of Chang'e 3 [16], and thus obtain $d < 1290$ mm, so we let $d = 1200$ mm for the following steps. Then, the normalization factor of the overall robot can be calculated by: $T = R_{ms}/t_2 = 1363.64/0.9 = 1515.15$ mm. So the optimum dimensional parameters of the overall robot can be obtained by: $l_3 = t_1 \cdot T = 909.09$ mm, $R_{sp} = t_3 \cdot T = 2272.73$ mm. Next, the normalization factor of the single leg can be ensured uniquely by: $R = l_3/r_1 = 909.09/2.5 = 363.64$ mm, so

the optimum dimensional parameters of the single leg can be obtained by: $b_1 = r_2 \cdot R = 327.27$ mm, $b_2 = r_3 \cdot R = 36.36$ mm, $a_1 = b_1 \cdot \chi = 490.91$ mm, $a_2 = b_2 \cdot \chi = 54.54$ mm. As a consequence, all dimensional parameters of the LML are optimized with the best comprehensive performance.

6 Conclusion

The paper proposes the optimum dimension design method for the Chang'e-Type Legged Mobile Lander, establishes a reliable and comprehensive optimization design model with proper mechanism topological parameters, performance criteria and constraint conditions. The study develops a systematic strategy to optimize both single leg and overall robot respectively. Finally, the relationship between different possible dimensions and the corresponding performances is analyzed, and the global optimum dimensions for the LML are obtained. The results shown by the performance atlases are perceptual and credible.

Acknowledgments. The author thanks the financial support under the projects from the National Natural Science Foundation of China (Grant No. 51735009) and the Research Fund of State Key Lab of MSV, China (Grant No. MSV-ZD-2016-08).

References

1. Orloff, R.W.: Apollo by the Numbers: A Statistical Reference for the Manned Phase of Project Apollo (2000)
2. Harvey, B.: Soviet and Russian Lunar Exploration. Praxis, New York (2007). <https://doi.org/10.1007/978-0-387-73976-2>
3. Li, C., Liu, J., Ren, X., et al.: The chang'e 3 mission overview. Space Sci. Rev. **190**(1–4), 85–101 (2015). <https://doi.org/10.1007/s11214-014-0134-7>
4. Birckenstaedt, B., Kutter, B.F., Zegler, F.: Centaur application to robotic and crewed lunar lander evolution. In: AIP Conference Proceedings, vol. 880, no. 1, p. 779 (2007). <https://doi.org/10.1063/1.2437517>
5. Mark, G.B.: A conceptual mars exploration vehicle architecture with chemical propulsion, near-term technology, and high modularity to enable near-term human missions to mars. In: AIAA SPACE 2015 Conference and Exposition, California, US (2015). <https://doi.org/10.2514/6.2015-4611>
6. Zhang, Z.X., Liang, L., Guo, L.L.: Concept of a wheeled-legged mobile manned lunar lander. Manned Space, 202–209 (2016). <https://doi.org/10.3969/j.issn.1674-5825.2016.02.010>
7. Yang, J.: Spacecraft Landing Buffer Mechanism. China Aerospace Publishing House, Beijing (2015)
8. NASA: Monte Carlo Approach to Touchdown Dynamics for Soft Lunar Landing, United States (1965)
9. NASA: A Mathematical Procedure for Predicting the Touchdown Dynamics of a Soft-Landing Vehicle, United States (1971)
10. NASA: Apollo Experience Report: Lunar Module Landing Gear Subsystem, United States (1972)

11. Wu, H., Wang, C., Ding, J., et al.: Soft Landing performance optimization of the new type lander based on multiple operating conditions. *J. Beijing Univ. Aeronaut. Astronaut.*, 1–7 (2016). <https://doi.org/10.13700/j.bh.1001-5965.2016.0296>
12. Gosselin, C., Angeles, J.: A global performance index for the kinematic optimization of robotic manipulators. *Trans. ASME. J. Mech. Des.* **113**(3), 220–226 (1991). <https://doi.org/10.1115/1.2912772>
13. Liu, X.J., Wang, J.S., Pritschow, G.: Performance atlases and optimum design of planar 5R symmetrical parallel mechanisms. *Mech. Mach. Theory* **41**(2), 119–144 (2006). <https://doi.org/10.1016/j.mechmachtheory.2005.05.003>
14. Papadopoulos, E., Rey, D.A.: The force-angle measure of tipover stability margin for mobile manipulators. *Vehicle Syst. Dyn.* **33**(1), 29–48 (2000). [https://doi.org/10.1076/0042-3114\(200001\)33:1;1-5;FT029](https://doi.org/10.1076/0042-3114(200001)33:1;1-5;FT029)
15. Liu, X.J., Wang, J.: A new methodology for optimal kinematic design of parallel mechanisms. *Mech. Mach. Theory* (2007). <https://doi.org/10.1016/j.mechmachtheory.2006.08.002>
16. Sun, Z., Zhang, T., Zhang, H., et al.: Technical design and achievements of Chang'e-3 probe. *China Sci. Technol. Sci.* (04), 331–343 (2014). <https://doi.org/10.1360/092014-37>